ANL/NDM--112

DE89 014105

ANL/NDM–112

SOME REMARKS ON THE NEUTRON ELASTIC– AND INELASTIC–SCATTERING CROSS SECTIONS OF PALLADIUM[†]

by

S. Chiba[††], P. T. Guenther, and A. B. Smith

May 1989

Keywords

Measured $d\sigma/d\Omega_{el}$ and $d\sigma/d\Omega_{inel}$. Incident neutrons ≈ $6-8$ MeV. Coupled–channels interpretation.

Engineering Physics Division
Argonne National Laboratory
9700 South Cass Avenue
Argonne, Illinois 60439
U. S. A.

[†] This work supported by the U.S. Department of Energy under Contract No. W–31–109–Eng–38.

[††] Permanent address, Japan Atomic Energy Research Institute, Tokai, Ibaraki, Japan.

NUCLEAR DATA AND MEASUREMENTS SERIES

The Nuclear Data and Measurements Series presents results of studies in the field of microscopic nuclear data. The primary objective is the dissemination of information in the comprehensive form required for nuclear technology applications. This Series is devoted to: a) measured microscopic nuclear parameters, b) experimental techniques and facilities employed in measurements, c) the analysis, correlation and interpretation of nuclear data, and d) the evaluation of nuclear data. Contributions to this Series are reviewed to assure technical competence and, unless otherwise stated, the contents can be formally referenced. This Series does not supplant formal journal publication but it does provide the more extensive information required for technological applications (e.g., tabulated numerical data) in a timely manner.

Additional copies [microfiche ($3.00) or xerographic (cost based on number of pages)] can be obtained by contacting:

NTIS Energy Distribution Center
P.O. Box 1300
Oak Ridge, TN 37831
U.S.A.
Comm. Phone: (614) 576–1301
FTS: 626–1301

TABLE OF CONTENTS

INFORMATION ABOUT OTHER ISSUES IN THE ANL/NDM SERIES

A list of titles and authors for reports ANL/NDM–1 through ANL/NDM–50 can be obtained by referring to any report of this Series numbered ANL/NDM–51 through ANL/NDM–76, while those for ANL/NDM–51 through ANL/NDM–76 are listed in any report numbered ANL/NDM–77 through ANL/NDM–101. Requests for a complete list of titles or for copies of previous reports should be directed to:

Section Secretary
Applied Nuclear Physics Section
Applied Physics Division
Building 316
Argonne National Laboratory
9700 South Cass Avenue
Argonne, Illinois 60439
U.S.A.

ANL/NDM–76 Alan B. Smith and Peter T. Guenther, *Scattering of Fast Neutrons from Elemental Molybdenum*, November 1982.

ANL/NDM–77 Donald L. Smith, *A Least–squares Method for Deriving Reaction Differential Cross Section Information from Measurements Performed in Diverse Neutron Fields*, November 1982.

ANL/NDM–78 A.B. Smith, P.T. Guenther and J.F. Whalen, *Fast–neutron Total and Elastic–scattering Cross Sections of Elemental Indium*, November 1982.

ANL/NDM–79 C. Budtz–Joergensen, P. Guenther, A. Smith and J. Whalen, *Few–MeV Neutrons Incident on Yttrium*, June 1983.

ANL/NDM–80 W.P. Poenitz and J.F. Whalen, *Neutron Total Cross Section Measurements in the Energy Region from 47 keV to 20 MeV*, July 1983.

ANL/NDM–81 D.L. Smith and P.T. Guenther, *Covariances for Neutron Cross Sections Calculated Using a Regional Model Based on Elemental–model Fits to Experimental Data*, November 1983.

ANL/NDM–82 D.L. Smith, *Reaction Differential Cross Sections from the Least–squares Unfolding of Ratio Data Measured in Diverse Neutrons Fields*, January 1984.

ANL/NDM–83 J.W. Meadows, *The Fission Cross Sections of Some Thorium, Uranium, Neptunium and Plutonium Isotopes Relative to* ^{235}U, October 1983.

ANL/NDM–84 W.P. Poenitz and J.W. Meadows, ^{235}U *and* ^{239}Pu *Sample–mass Determinations and Intercomparisons*, November 1983.

ANL/NDM–85 D.L. Smith, J.W. Meadows and I. Kanno, *Measurement of the* $^{51}V(n,p)^{51}Ti$ *Reaction Cross Section from Threshold to 9.3 MeV*, June 1984.

ANL/NDM–86 I. Kanno, J.W. Meadows and D.L. Smith, *Energy– differential Cross–section Measurement for the* $^{51}V(n,\alpha)^{48}Sc$ *Reaction*, July 1984.

ANL/NDM–87 D.L. Smith, J.W. Meadows, M.M. Bretscher and S.A. Cox, *Cross–section Measurement for the* $^{7}Li(n,n't)^{4}He$ *Reaction at 14.74 MeV*, September 1984.

ANL/NDM–88 A.B. Smith, D.L. Smith and R.J. Howerton, *An Evaluated Nuclear Data File for Niobium*, March 1985.

ANL/NDM–89 Bernard P. Evain, Donald L. Smith and Paul Lucchese, *Compilation and Evaluation of 14–MeV Neutron–activation Cross Sections for Nuclear Technology Applications: Set I*, April 1985.

ANL/NDM–90 D.L. Smith, J.W. Meadows and P.T. Guenther, *Fast–neutron–spectrum Measurements for the Thick–target* $^{9}Be(d,n)^{10}B$ *Reaction at* $E_{\rm d} = 7$ *MeV*, April 1985.

ANL/NDM–91 A.B. Smith, P.T. Guenther and R.D. Lawson, *On the Energy Dependence of the Optical Model of Neutron Scattering from Niobium*, May 1985.

ANL/NDM–92 Donald L. Smith, *Nuclear Data Uncertainties (Vol–I): Basic Concepts of Probability*, April 1986.

ANL/NDM–93 D.L. Smith, J.W. Meadows and M.M. Bretscher, *Integral Cross–section Measurements for* $^{7}Li(n,n't)^{4}He$, $^{27}Al(n,p)^{27}Mg$, $^{27}Al(n,\alpha)^{24}Na$, $^{58}Ni(n,p)^{58}Co$, *and* $^{60}Ni(n,p)^{60}Co$ *Relative to* ^{238}U *Neutron Fission in the Thick–target* $^{9}Be(d,n)^{10}B$ *Spectrum at* $E_{\rm d} = 7$ *MeV*, October 1985.

ANL/NDM–94 A.B. Smith, D.L. Smith, P. Rousset, R.D. Lawson and R.J. Howerton, *Evaluated Neutronic Data File for Yttrium*, January 1986.

ANL/NDM–95 Donald L. Smith and James W. Meadows, *A Facility for High–intensity Neutron Irradiations Using Thick–target Sources at the Argonne Fast–neutron Generator*, May 1986.

ANL/NDM–96 M. Sugimoto, A.B. Smith and P.T. Guenther, *Ratio of the Prompt–fission–neutron Spectrum of Plutonium–239 to that of Uranium–235*, September 1986.

ANL/NDM–97 J.W. Meadows, *The Fission Cross Sections of* ^{230}Th, ^{232}Th, ^{233}U, ^{234}U, ^{236}U, ^{238}U, ^{237}Np, ^{239}Pu, *and* ^{242}Pu *Relative* ^{235}U *at 14.74 MeV Neutron Energy*, December 1986.

ANL/NDM–98 J.W. Meadows, *The Fission Cross Section Ratios and Error Analysis for Ten Thorium, Uranium, Neptunium and Plutonium Isotopes at 14.74–MeV Neutron Energy*, March 1987.

ANL/NDM–99 Donald L. Smith, *Some Comments on the Effects of Long–range Correlations in Covariance Matrices for Nuclear Data*, March 1987.

ANL/NDM–100 A.B. Smith, P.T. Guenther and R.D. Lawson, *The Energy Dependence of the Optical–model Potential for Fast–neutron Scattering from Bismuth*, May 1987.

ANL/NDM–101 A.B. Smith, P.T. Guenther, J.F. Whalen and R.D. Lawson, *Cobalt: Fast Neutrons and Physical Models*, July 1987.

ANL/NDM–102 D. L Smith, *Investigation of the Influence of the Neutron Spectrum in Determinations of Integral Neutron Cross–Section Ratios*, November 1987.

ANL/NDM–103 A.B. Smith, P.T. Guenther and B. Micklich, *Spectrum of Neutrons Emitted From a Thick Beryllium Target Bombarded With 7 MeV Deuterons*, January 1988.

ANL/NDM–104 L.P. Geraldo and D.L. Smith, *Some Thoughts on Positive Definiteness in the Consideration of Nuclear Data Covariance Matrices*, January 1988.

ANL/NDM–105 A.B. Smith, D.L. Smith, P.T. Guenther, J.W. Meadows, R.D. Lawson, R.J. Howerton, and T. Djemil, *Neutronic Evaluated Nuclear–Data File for Vanadium*, May 1988.

ANL/NDM–106 A.B. Smith, P.T. Guenther, and R.D. Lawson, *Fast–Neutron Elastic Scattering from Elemental Vanadium*, March 1988.

ANL/NDM–107 P. Guenther, R. Lawson, J. Meadows, M. Sugimoto, A. Smith, D. Smith, and R. Howerton, *An Evaluated Neutronic Data File for Elemental Cobalt*, August 1988.

ANL/NDM–108 M. Sugimoto, P.T. Guenther, J.E. Lynn, A.B. Smith, and J.F. Whalen, *Some Comments on the Interaction of Fast–Neutrons with Beryllium*, November 1988.

ANL/NDM–109 P.T. Guenther, R.D. Lawson, J.W. Meadows, A.B. Smith, D.L. Smith, and M. Sugimoto, *An Evaluated Neutronic Data File for Bismuth*, March 1989 (not yet printed)

ANL/NDM–110 D.L. Smith and L.P. Geraldo, *A Vector Model for Error Propatation*, March 1989.

ANL/NDM–111 J.E. Lynn, *Fifty Years of Nuclear Fission*, June 1989.

SOME REMARKS ON THE NEUTRON ELASTIC– AND INELASTIC–SCATTERING CROSS SECTIONS OF PALLADIUM[†]

by

S. Chiba[††], P. T. Guenther, and A. B. Smith

ABSTRACT

The cross sections for the elastic–scattering of 5.9, 7.1 and 8.0 MeV neutrons from elemental palladium were measured at forty scattering angles distributed between ≈ 15° and 160°. The inelastic–scattering cross sections for the excitation of palladium levels at energies of 260 keV to 560 keV were measured with high resolution at the same energies, and at a scattering angle of 80°. The experimental results were combined with lower–energy values previously obtained by this group to provide a comprehensive data base extending from near the inelastic–scattering threshold to 8 MeV. That data base was interpreted in terms of a coupled–channels model, including the inelastic excitation of one– and two–phonon vibrational levels of the even isotopes of palladium. It was concluded that the palladium inelastic–scattering cross sections, at the low energies of interest in assessment of fast–fission–reactor performance, are large (≈ 50% greater than given in widely used evaluated fission–product data files). They primarily involve compound–nucleus processes, with only a small direct–reaction component attributable to the excitation of the one–phonon, 2^+, vibrational levels of the even isotopes of palladium.

[†] This work supported by the U.S. Department of Energy under Contract No. W–31–109–Eng–38.

[††] Permanent address, Japan Atomic Energy Research Institute, Tokai, Ibaraki, Japan.

I. INTRODUCTION

Fission products are found primarily in two groups centered about mass A = 95 and A = 140. Inelastic–neutron excitation of collective low–lying levels is a concern in both mass regions (in the former the excitation of dynamic–vibrational levels, and in the latter that of rotational levels). The cross sections for the neutron excitation of such low–lying collective levels can be large. A consequence of these processes is appreciable energy transfer in FBR spectra, resulting in significant sensitivity of the macroscopic neutronic system to the magnitude of fission–product neutron inelastic–scattering cross sections. For the prominent fission products, this sensitivity can be ≈ 25% that of the neutron capture process.[1] Very recently there has been speculation about the "cold" fusion of deuterium imbedded in the lattice of palladium metal.[2] In the event that such a phenomenon can be used for energy generation, the neutron cross sections of palladium will be essential to the design of a practical energy system. Thus, the magnitudes of the cross sections for the neutron excitation of the collective modes of palladium are an applied concern.

The above neutron inelastic–scattering cross–section strength is primarily the result of compound–nucleus (CN) processes,[3] to which is added a direct collective–excitation component.[4-5] The even palladium isotopes are prominent light–mass fission products, and they display the characteristics of strong collective vibrators, with β_2 in the ≈ 0.20 – 0.26 range.[6] It has been suggested that the neutron direct–vibrational excitation of their first, 2^+ one–phonon, levels is large, which, together with the conventional compound–nucleus contribution, results in very large neutron inelastic–scattering cross sections at low incident energies.[4+7] There is some support of this thesis in the results from (n;n',γ) measurements.[5] On the other hand, the results of direct (n,n') measurements are generally consistent with a relatively small direct component.[8] These inelastic–scattering uncertainties extend to neighboring prominent fission products, for example, to the even isotopes of ruthenium.

The present study addresses the above issue with measurements of the cross sections for the excitation of the one–phonon, 2^+, levels of the even isotopes of palladium, and for neutron elastic–scattering from palladium, up to incident–neutron energies of 8 MeV, coupled with an interpretation of the experimental results using optical–statistical and coupled–channels models.

II. EXPERIMENTAL METHODS

The present measurements employed a solid cylinder of elemental metallic palladium, 2 cm long and 2 cm in diameter. The D(d,n)^{3}He reaction was used as the neutron source, with the deuterium gas contained in a cell 3 cm long. The deuterium gas pressure in the cell was adjusted to give neutron energy spreads at the sample ranging from 50 to 200 keV (including effects due to reaction kinematics), depending on the desired incident–neutron energy resolution. The mean energy of the incident neutrons was determined to 25 – 50 keV by control of the energy of the incident deuteron beam. The neutron source was pulsed at a repetition rate of 2 MHz, with a burst duration of approximately 1 nsec. All of the measurements used the fast–neutron time–of–flight method. Scattered–neutron angular distributions were obtained using the Argonne ten–angle time–of–flight[9] system, with flight paths of ≈ 5 m. The high–resolution measurements were made at an 80° scattering angle with a flight path of 15.68 m. The details of these instrumental arrangements have been described elsewhere.[9,10,11]

The cross sections were all measured relative to the well–known H(n,n) scattering standard.[12] The relative detector sensitivities were established using the ^{252}Cf fission–neutron spectrum, as described in Ref. 13. The relative scattering angles were optically determined to accuracies of better than 0.1°. The normalization of the relative angular scale was achieved by observing elastic–neutron scattering from a heavy target (usually niobium), left and right of the apparent angle center line, at angles where the elastic–scattering cross section is rapidly changing with the angle. This method gave results that were reproducible to 0.15°. The measured values were corrected for angular–resolution, multiple–event and neutron–attenuation effects using Monte–Carlo methods.[14] A large number of histories and three iterations were used, so as to provide corrections to 1–2% accuracy, except at the very deep first minimum of the elastic distributions where the uncertainties in the correction factors may be 10% or more. Cross–section uncertainties due to counting statistics (including both foreground and background) varied from less than 1% to several percent depending on the flight path and scattering angle. Relative detector sensitivities were reproducible to better than 3%, and were independently determined for each of the detectors. The above–cited angular uncertainties introduced significant cross–section uncertainty in regions of rapidly changing cross section (e.g., the rapidly changing elastic–scattering cross section at forward scattering angles). These various uncertainty components were combined in quadrature to obtain the total uncertainties. Generally, the results of measurements with different detectors, or made at different times, were consistent to within the respective uncertainties.

III. EXPERIMENTAL RESULTS

The angular distributions of scattered neutrons were measured at 5.9, 7.1, and 8.0 MeV, for forty angles distributed between 15° and 160°, using the 5 m flight paths. With those flight paths, the neutrons resulting from the excitation of low–lying levels were only partially resolved from the elastically–scattered component at scattering angles larger than ≈ 50°, and they were not at all resolved at more forward angles. Therefore, in the angular–distribution measurements, inelastically–scattered contributions corresponding to excitations of $\lesssim$ 560 keV (i.e., mainly those due to the excitation of the 2^+ vibrational levels of the even isotopes of palladium) were intentionally included with the elastically–scattered components at all measurement angles. Herein, these composite angular distributions are referred to as "pseudo" elastic scattering. The measured values gave good definition of the pseudo elastic scattering, as illustrated in Fig. 1.

The differential cross sections for excitation of levels in palladium in the range 260 - 560 keV were measured at 5.9, 7.1, and 8.0 MeV, at a scattering angle of 80°, using the 15.68 m flight path. The experimental resolution was sufficient to separate these inelastic components from elastically–scattered neutrons, as illustrated by the time–of–flight spectrum of Fig. 2. A prominent feature of Fig. 2 is the inelastically–scattered neutron group primarily due to excitations of levels in the range ≈ 260 – 560 keV. These are very largely the result of contributions from the 2^+, one–phonon, vibrational states of the even isotopes of palladium, with a relatively small addition of contributions due to the odd isotope ^{105}Pd (≈ 22.3% abundant). In addition, there is a small "tail" on the inelastic peak corresponding to the excitation of a number of higher–lying levels in ^{105}Pd. The

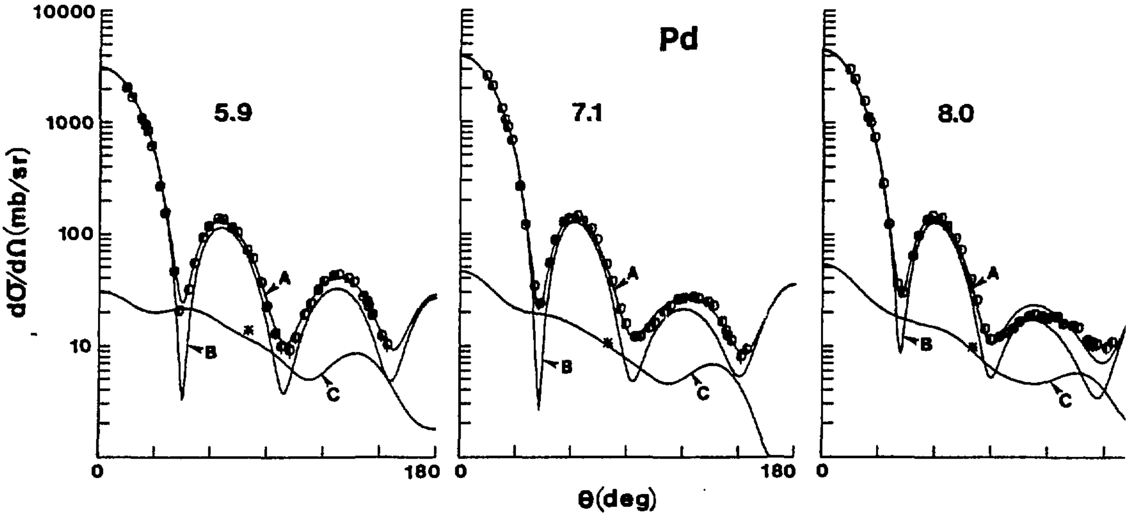

Fig. 1. Differential elastic– and inelastic–scattering cross sections of palladium measured at 5.9, 7.1, and 8.0 MeV, as numerically noted. The "O" symbols indicate pseudo elastic–scattering results, inclusive of contributions from neutrons due to the excitation of levels up to ≈ 560 keV. The "X" symbols indicate the cross sections for the inelastic excitation of levels in the range 260 – 560 keV. The curves indicate the results of model calculations, as described in the text. The data are given in the laboratory–coordinate system

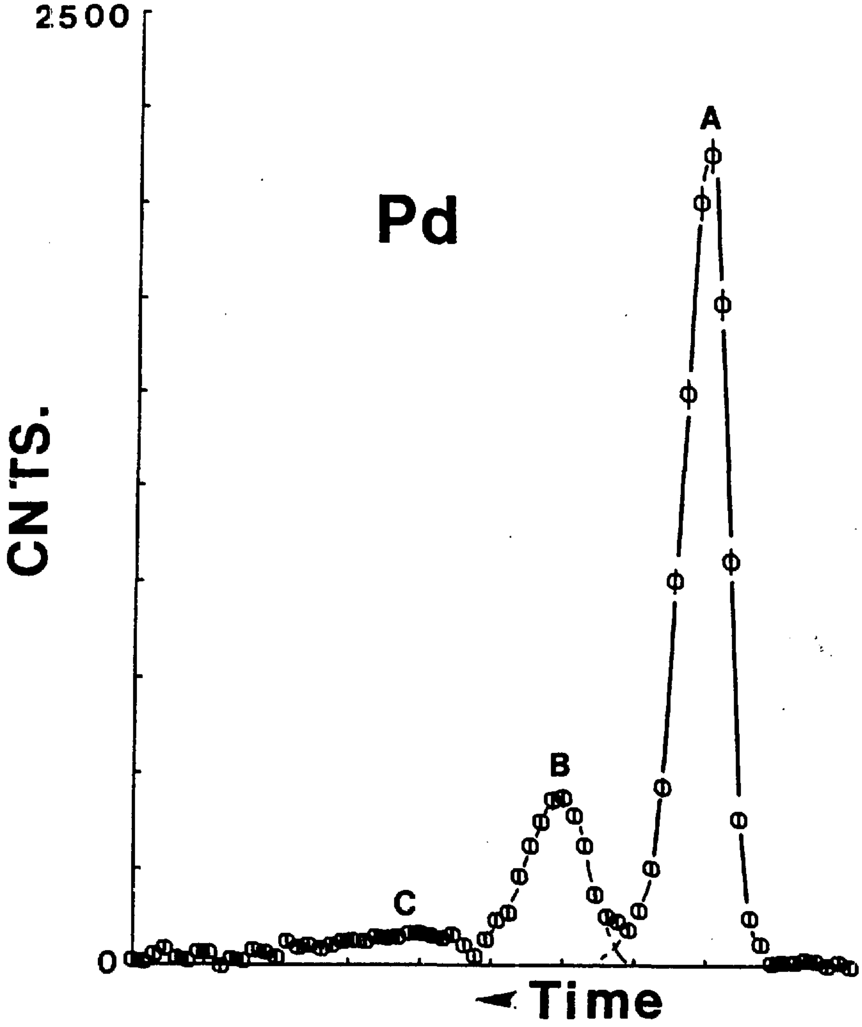

Fig. 2. An experimental time–of–flight spectrum obtained by scattering 7.1 MeV neutrons from elemental palladium, at an angle of 80°, over a flight path of 15.68 m. Components of the spectrum are noted as: (A) the elastically–scattered group, (B) inelastically–scattered neutrons corresponding to excitations of ≈ 260 – 560 keV, primarily due to the even isotopes of palladium, and (C) low–intensity inelastically–scattered neutrons due to the excitation of a number of levels above ≈ 560 keV in ^{105}Pd.

corresponding differential cross sections are given in Table 1. The uncertainties associated with these differential inelastic–scattering cross sections consisted of the above–cited components and subjective estimates of the uncertainties involved in summing the time–of–flight spectra, such as illustrated by the dashed curves in Fig. 2. The resulting total uncertainties were ≈ 10%, and the results deduced at separate times were consistent with this value. These inelastic–scattering cross sections extrapolate reasonably well to the lower–energy values obtained in the previous work of Ref. 8, as described below.

Table 1

The 80° neutron differential inelastic–scattering cross sections corresponding to the excitation of ≈ 260 – 560 keV levels in elemental palladium.

Incident Energy (MeV)	$d\sigma/d\Omega$ (mb) at 80°
5.9	13.8
7.1	10.7
8.0	9.8

IV. INTERPRETATION

Neutron total cross sections are measurable in a self–normalizing manner, and unambiguously calculable with optical or coupled–channels models. Thus, they are a consideration in the interpretation of the interaction of fast neutrons with palladium. There is an extensive body of palladium neutron total cross sections, largely as the result of work by this group.[8,15] These data, augmented with the files of the National Nuclear Data Center, provided a detailed neutron total–cross–section data base, extending from below the threshold for inelastic–neutron scattering to above 10 MeV. The components of this data base were inspected on large–scale graphs; obviously erroneous data were abandoned, and the remaining values were averaged over 200 keV energy increments in order to obtain the energy–averaged neutron total cross sections shown in Fig. 3. These energy–averaged neutron total cross sections are comparable to the predictions of a coupled–channels model.

The elastic–scattering data base used in the interpretation consisted of the present results and the lower–energy values of Ref. 8. As described above, the present pseudo elastic–scattering results included inelastically–scattered components corresponding to excitations of up to $E_x = 560$ keV. This composite nature of the distributions was taken into account in the calculations as discussed below. The results of the lower–energy elastic–scattering measurements of Ref. 8 consist of ≈ 45 angular distributions, distributed between 1.5 and 3.8 MeV, all resolving the elastically–scattered component from

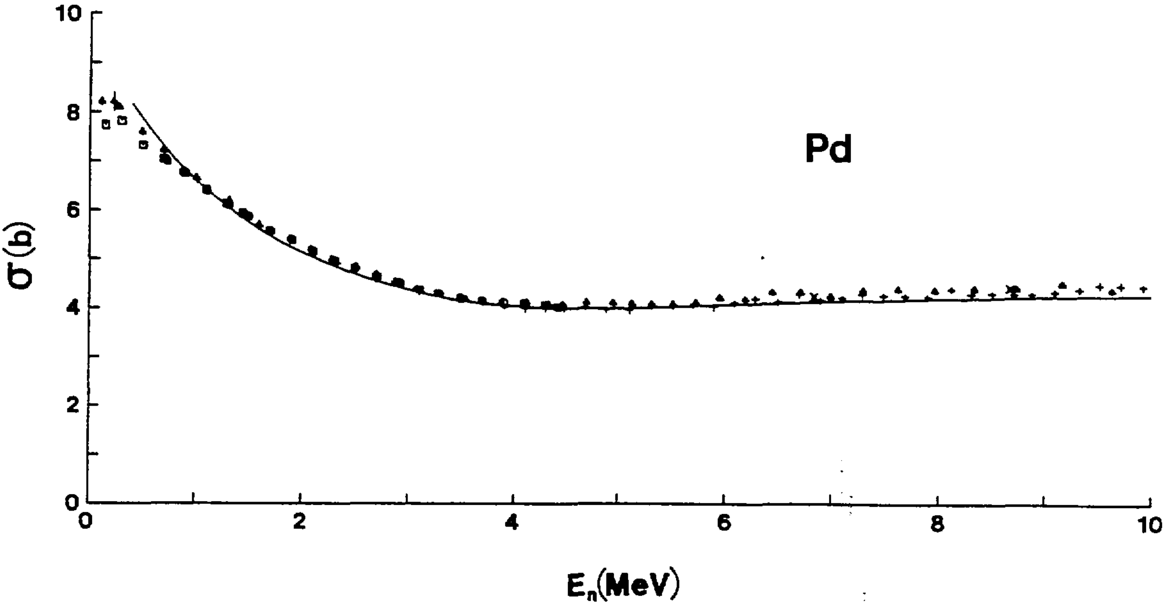

Fig. 3. The neutron total–cross–section data base for palladium. Symbols indicate energy–averaged experimental values deduced from individual data sets, as described in the text. The curve shows the result of the coupled–channels interpretation discussed in the text.

inelastically–scattered contributions. These lower–energy results were averaged over ≈ 0.2–MeV energy intervals in order to smooth any residual fluctuations and to reduce the number of distributions subject to extensive numerical fitting procedures. There are a few other palladium elastic–scattering results, notably the data of Ref. 16 (below 1.5 MeV). These additional data were not used in the present interpretation, since the results are old and not up to contemporary standards and/or are at very low energies where the data fluctuations due to partially–resolved resonance structure may be relatively large and where the distributions are of a rather structureless character that does not particularly define a model. The elastic–scattering data base used in the interpretation is summarized by the measured values shown in Figs. 1 and 4.

The neutron inelastic–scattering data were compared with the predictions of the coupled–channels model deduced from the elastic–scattering data. The inelastic–scattering data were composed of the lower–energy angle–integrated values from prior work at this laboratory[8] and the 80° differential values of the present work as given in Table 1. Only inelastic excitations of $\lesssim$ 560 keV were considered, since these are the components of primary interest from the points of view of large fission–product inelastic–scattering cross sections and of direct excitation of the 2^+, one–phonon, vibrational states of the even isotopes of palladium.

The interpretation assumed a coupled–channels model having a real Saxon–Woods potential, a derivative Saxon–Woods imaginary potential, and a spin–orbit potential of the Thomas form.[17] The spin–orbit potential was fixed at a strength of 6.0 MeV, a radius of 1.26 fm, and a diffuseness of 0.636 fm. These spin–orbit potential values were found to be very suitable in the lower–energy interpretations of Ref. 8. Elemental palladium consists ≈ 80% of even isotopes having similar low–lying vibrational levels. Predominant among these are ^{106}Pd (27.3%) and ^{108}Pd (26.5%). Thus, the interpretation assumed that the element was reasonably represented by ^{106}Pd. Above ≈ 4.0 MeV, the level density of ^{106}Pd is large, and thus compound–elastic (CE) contributions to the elastic scattering at the energies of the present experiments are expected to be small. This expectation is supported by the very deep minima of the elastic–scattering angular distributions, even at 4.0 MeV.[8] Thus, it was assumed that elastic scattering at 7.1 and 8.0 MeV could be treated as an entirely shape–elastic (SE) process. At energies of 5.9 MeV and below, the observed elastic–scattering cross sections were corrected for CE contributions using the spherical optical–statistical model (SOM) of Ref. 8. The SOM employed 20 discrete ^{106}Pd levels extending to an excitation energy of ≈ 2.4 MeV,[18] and the statistical formulation of Gilbert and Cameron[19] to describe higher–energy excitations. The SOM calculations included the width–fluctuation and correlation corrections of Moldauer.[3] The resulting CE corrections were small, even at 1.5 MeV. This correction procedure was an approximation, since it was based upon SOM transmission coefficients rather than the transmission coefficients of the vibrational coupled–channels model. However, use of the coupled–channels–model transmission coefficients changed the corrections at the minima of the lowest–energy (1.5 MeV) distribution by only 5.5%, thus reasonably justifying the use of the simpler SOM model. The observed lower–energy elastic–scattering data of Ref. 8, and the pseudo elastic–scattering data of the present measurements (corrected for the CE contributions) were the basis for chi–square fitting to determine the real and imaginary potential parameters of the coupled–channels model.

The chi–square coupled–channels–model fitting concurrently varied the four parameters (real and imaginary strengths and diffusenesses) while keeping the radii fixed. A number of choices of radii were explored with no significant improvement in the fitting

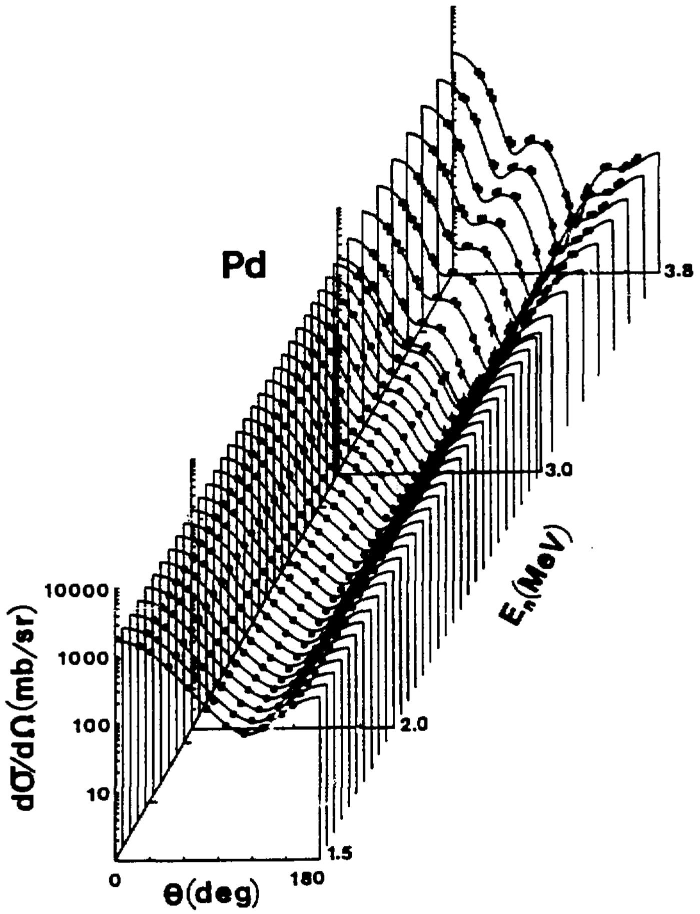

Fig. 4. Differential elastic–scattering cross sections of palladium from 1.5 to 3.8 MeV. The measured values of Ref. 8 are indicated by "O" symbols, and the curves indicate results from coupled–channels calculations (including CN contributions), as described in the text. The data are given in the laboratory–coordinate system.

results (assessed either by chi–square or subjective judgment) over the radii obtained in the extensive lower–energy fitting of Ref. 8. Therefore, the real ($r_v = 1.260$ fm) and imaginary ($r_w = 1.231$ fm) radii of Ref. 8 were accepted for all subsequent four–parameter fitting. (Throughout this discussion, radii are expressed in the form $R_i = r_i \cdot A^{1/3}$, where A is the target mass number). The fitting was carried out using the coupled–channels code ANLECIS,[20] and was entirely confined to the elastic–scattering data base outlined above. In fitting the pseudo elastic–scattering data at 5.9, 7.1, and 8.0 MeV, the composite distribution of elastic–scattering and inelastic–scattering due to the excitation of the 0.5118 MeV, 2^+ one–phonon, level was explicitly calculated and used in the fitting. A one– and two–phonon coupling scheme was assumed, consisting of the 0.5118 (2^+) MeV, and 1.1279 (2^+), 1.1336 (0^+), 1.2289 (4^+) MeV levels, respectively.[18] Various values of β_2 were examined. The sensitivity of the fitting results to β_2 was not very great, but a value of $\beta_2 = 0.25$ generally resulted in smaller chi–squares and was therefore accepted for subsequent fitting. This value of β_2 is ≈ 10% larger than deduced from coulomb–excitation studies.[6]

The results of the four–parameter data fitting were descriptive of the observed data as is illustrated by the examples given in Fig. 5. The parameters resulting from the four–parameter fitting followed a general linear energy dependence. This behavior was least–square fitted to obtain the energy–dependencies of the potential parameters given in Eq. (1).

$$\begin{array}{lcll} V & = & \left[46.991(\pm 0.215) - 0.207(\pm 0.062)\cdot E\right] & \text{MeV} \\ a_v & = & \left[0.598(\pm 0.012) + 0.010(\pm 0.003)\cdot E\right] & \text{fm} \\ W & = & \left[4.047(\pm 0.701) + 0.604(\pm 0.172)\cdot E\right] & \text{MeV} \\ a_w & = & \left[0.572(\pm 0.037) - 0.014(\pm 0.009)\cdot E\right] & \text{fm,} \end{array} \qquad (1)$$

where E is the incident energy in MeV, V the real–potential strength, a_v the real–potential diffuseness, W the imaginary–potential strength, and a_w the imaginary–potential diffuseness. The real–potential strength falls with energy, as indicated by the Hartree–Fock predictions,[17] and the imaginary–potential strength increases with energy, as one would expect, due to the increasing contributions of levels not explicitly considered. The diffusenesses (a_v and a_w) have a small energy dependence that may be correlated with the fixed radii assumed in the fitting procedures. The detailed examination of the relation between radii and diffusenesses would require a far more comprehensive data base (and associated fitting) than presently available. Qualitatively, the energy dependencies of the potential strengths follow the trends of "global" models.[21] The general potential of Eq. (1), while not giving as detailed a description of the experimental values as the explicit fits shown in Fig. 5, results in calculated cross sections in reasonably good agreement with the experimental results, as illustrated by the curves in Figs. 1 and 4. In the former figure, the "B" curve indicates the calculated elastic scattering, while the "A" curve shows the calculated pseudo elastic–scattering, inclusive of the contributions due to the inelastic-

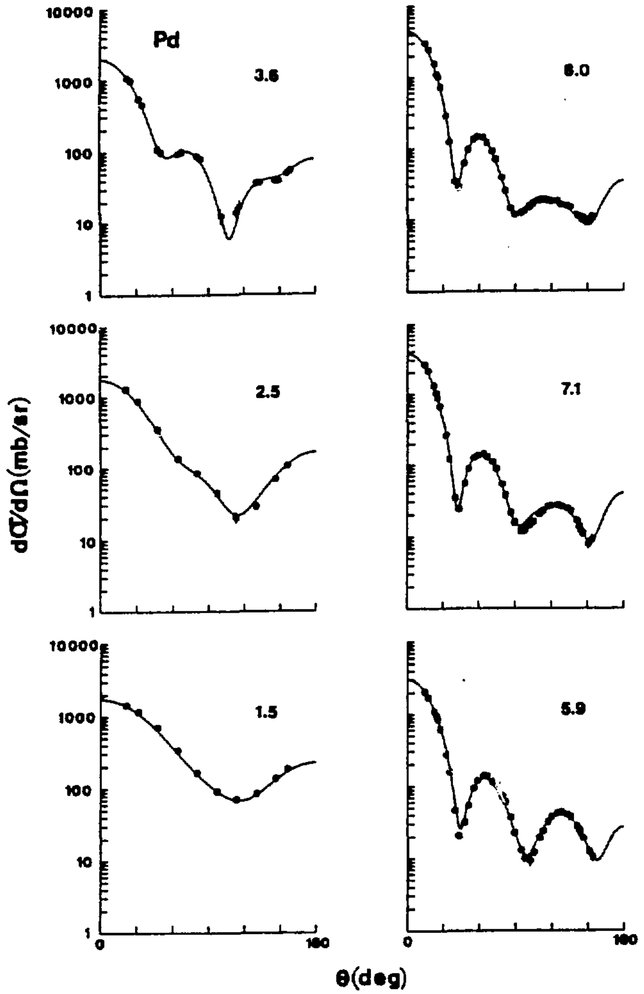

Fig. 5. Illustrative comparisons of measured and calculated elastic–scattering distributions. Below 4.0 MeV the results refer to elastic scattering, and at higher energies to "pseudo" elastic–scattering, as defined in the text. Symbols indicate the measured values, and curves the results of four–parameter fitting. The incident–neutron energies (in MeV) are numerically given in each section of the figure. The data are given in the laboratory–coordinate system.

excitation of the 0.5118 (2^+) MeV level. The only substantive difference is at the highest, 8.0 MeV, energy, and even then only near the minima of the distribution and involving a magnitude of only a few mb/sr. At this highest energy, the assumed coupling scheme may well be an oversimplification, and the coupling of additional levels could change the details of the distribution in the very small minima. Such detailed coupling schemes require a knowledge of the respective nuclear structure that is not available, and even if it were would lead to very tedious calculations.

Fitting the neutron inelastic excitation of the first 2^+ vibrational level was not a major consideration in the derivation of the above potential, though it did support the selected β_2 value. However, the model provides calculated cross sections that are comparable to the experimental values, as illustrated in Figs. 1 and 6. Throughout the comparisons of measured and calculated inelastic–scattering cross sections, compound nucleus contributions were added to the direct inelastic scattering in a manner analogous to that used in determining the CE corrections cited above. These corrections were significant only at 5.9 MeV and lower energies. The high–resolution 80° inelastic–scattering results of the present work at 5.9, 7.1, and 8.0 MeV are in remarkable agreement with the calculated results, as illustrated in Fig. 1. Therefore, it is reasonable to use the calculated angular distributions (curves "C" of Fig. 1), normalized to the measured 80° values, to obtain the angle–integrated inelastic–scattering cross sections. These angle–integrated results are shown in Fig. 6, together with the lower–energy results of Ref. 8. The calculated direct inelastic scattering rises slowly from the threshold to a general plateau, as illustrated by curve "B" of Fig. 6. Curve "A" of Fig. 6 indicates the total inelastic–scattering cross section for the excitation of the 0.5118 MeV level. The large maximum at ≈ 1.0 MeV consists very largely of CN contributions. The calculated cross sections are at the lower extreme of the uncertainties of the lower–energy data of Ref. 8. The uncertainties in the respective data of Ref. 8 are, to a very large extent, systematic, since the measurements used the ^{7}Li(p,n)^{7}Be neutron source which has a prominent second neutron group due to the ^{7}Li(p,n)^{7}Be* reaction that seriously distorts the observation of neutrons due to the inelastic excitation of levels near 500 keV. As a consequence, substantial corrections had to be made to derive the respective cross sections of Ref. 8. Thus, the systematic cross–section uncertainties were large, and it is not surprising that the present calculated inelastic cross sections are at the lower extreme of the uncertainties of the data of Ref. 8. Generally, the measured and/or calculated cross sections for the inelastic neutron excitation of ≈ 260 – 560 keV levels in palladium do not rise to more than 1.2 –1.3 b at the maximum at ≈ 1.0 MeV, and in this region the cross sections are very largely due to CN processes. The contribution due to direct processes at lower energies is small.

The above model gives a reasonable description of the neutron total cross section from the inelastic–scattering threshold to more than 8.0 MeV, as shown in Fig. 3. Over this wide energy region, the calculations agree with the measured values to within several percent, a difference that is frequently comparable to that between the various experimental data sets. At very low energies the calculations tend to be systematically larger than the measured values, but the latter may be distorted toward too small magnitudes due to self–shielding. The strength functions of palladium isotopes deduced from resonance measurements vary by a factor of two or more, depending on the isotopes involved.[22] The model predicts $S_0 = (0.94 \times 10^{-4})$ and $S_1 = (5.7 \times 10^{-4})$. These are reasonably consistent with the ^{108}Pd values of $(0.78 \pm 0.17) \times 10^{-4}$ and $(4.4 \pm 0.5) \times 10^{-4}$, respectively, given in Ref. 22. However, S_0 for ^{106}Pd, deduced from resonance data, is

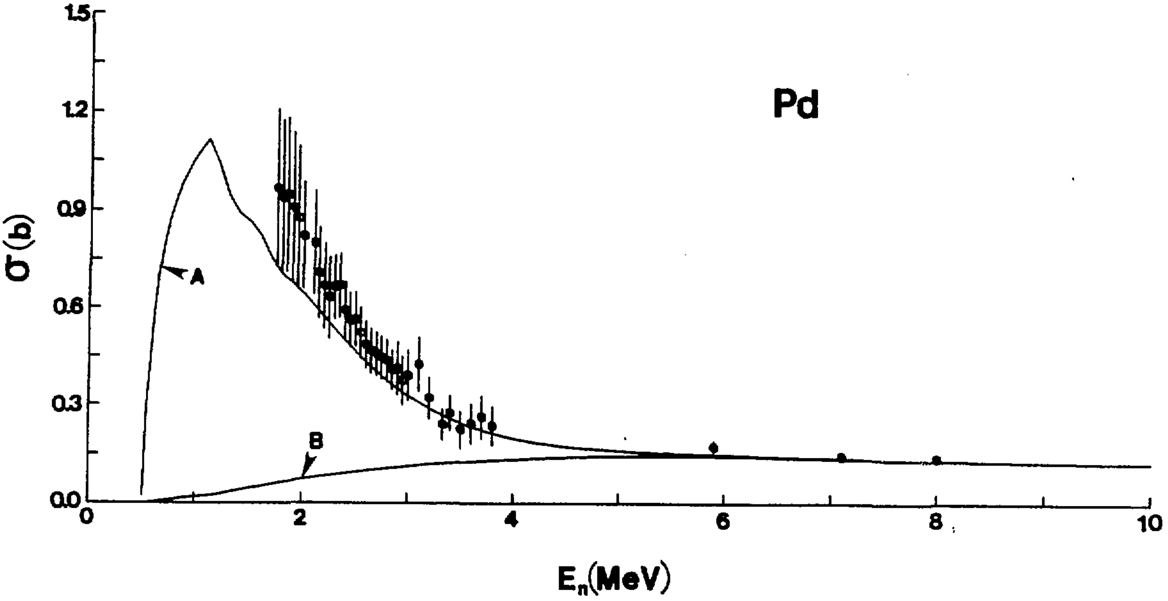

Fig. 6. Comparison of measured and calculated angle–integrated cross sections for the neutron excitation of 0.260 – 560 keV levels in palladium. The symbols indicate measured values: below 4.0 MeV from Ref. 8, and above 5.0 MeV from the present work, as described in the text. The curves indicate calculated results where "B" is the direct–reaction component and "A" the total inelastic cross section inclusive of direct–reaction and CN contributions.

(0.34 ± 0.04) x 10^{-4}.[22] Given these large differences from isotope to isotope, comparison with model–predicted strength functions is not too rewarding.

V. DISCUSSION

The above interpretation is, in part, based upon the assumption that inelastic neutron scattering is similar for each of the even isotopes of palladium. The element consists of nearly 80% even isotopes that have very similar low–lying excited structure and β_2 values.[6+18] Using the above model, the inelastic cross sections for the excitation of the first, 2^+, level of each isotope were calculated and combined to obtain an "elemental" cross section consisting of only even isotopes. The result was very similar to that obtained for ^{106}Pd alone (e.g., at 2.0 MeV the "elemental" CN cross section was 540 mb, compared to 565 mb for ^{106}Pd alone). The only odd isotope, ^{105}Pd, is 22.3% abundant. It probably has nine excited states below ≈ 560 keV,[18+23] all of which contribute to the inelastic–scattering cross sections observed in the present experiments. A model of ^{105}Pd is that of a $d_{5/2}$–hole coupled to the low–lying states of ^{106}Pd. To the extent to which the ^{105}Pd states below 560 keV can be thought of as a $d_{5/2}$–hole coupled to the 511.8 keV 2^+ state of ^{106}Pd, the low–energy inelastic–scattering cross sections of ^{105}Pd should be the same as those of ^{106}Pd. Furthermore, the dominant inelastic scattering in this odd–A nucleus almost certainly comes from the excitation of states involving just this coupling mode. The only member of the quintet of spins ($1/2^+$, $3/2^+$, $5/2^+$, $7/2^+$, and $9/2^+$), arising from the ($d_{5/2}^{\bullet}$,2^+) coupling, for which no candidate is seen below 560 keV, is the $9/2^+$ level. Thus, probably about 2/3 of the ^{106}Pd inelastic–scattering cross section has been seen in ^{105}Pd. Since ^{105}Pd is only 22.3% abundant in the natural palladium target, the approximation of replacing its inelastic–scattering contribution by that of ^{106}Pd will not substantially alter the calculated elemental results.

The present measurements and their interpretation strongly suggest that the inelastic–scattering cross sections of palladium, at the lower energies of importance, in the context of fission products and fission–reactor performance, are very largely due to conventional CN processes. The cumulative inelastic–scattering cross section for the excitation of levels up to ≈ 560 keV peaks at about 1.2 b near an incident energy of 1.0 MeV, and then rapidly falls as the energy increases. The measurements and their interpretation also indicate that the direct inelastic excitation of the first, 2^+, vibrational level of the predominant even isotopes of palladium (E_x ≈ 500 keV) rises slowly from threshold to a maximum of ≈ 150 mb at 6.0 MeV. Thus, direct inelastic–scattering processes in palladium are of little concern in the fission–reactor context. However, the present experiments and their interpretation very much support magnitudes of the inelastic–scattering cross sections of palladium at the lower energies of fission–reactor concern (e.g., from threshold to several MeV) that are ≈ 50% larger than found in widely used evaluated nuclear data files (e.g., as given by ENDF/B–V[24]). This difference between measured and evaluated inelastic–scattering cross sections has been pointed out as a result of previous work at this laboratory.[9]

ACKNOWLEDGMENTS

The authors are very much indebted to Dr. R. D. Lawson for a number of helpful comments and suggestions.

REFERENCES

1. H. Gruppelaar, R. Heijboer, A. Jansen, H. Van der Kamp, N. Karouby–Cohen, L. Martin–Deidier, G. Rimpault, and M. Salvatores, Proc. Inter. Conf. on Nuclear Data for Basic and Applied Science, P. Young, R. Brown, G. Auchampaugh, P. Lisowski and L. Stewart, Eds., Gordon and Breach Science Pub., New York p. 1537 (1986).

2. B. S. Pons and M. Fleischmann, TIME, May 8, p. 72 (1989)

3. P. A. Moldauer, Nucl. Phys. A344 185 (1980).

4. H. Gruppelaar and H. Van der Kamp, Proc. Specialist's Mtg. on Use of the Optical Model for the Calculation of Neutron Cross Sections below 20 MeV, NEANDC Report NEANDC–222'U', NEA Press, Paris, p. 221 (1986).

5. E. Konobeevskii and V. Popov, Sov. J. Nucl. Phys. 33 7 (1981).

6. S. Raman, C. H. Malarkey, W. T. Milner, C. W. Nestor, Jr., and P. H. Stelson, Atomic and Nuclear Data Tables 36 1 (1987).

7. H. Gruppelaar, informal presentation at the IAEA coordinated research project on the calculation of structural material nuclear data, Vienna (1988).

8. A. Smith, P. Guenther, and J. Whalen, Argonne National Laboratory Report, ANL/NDM–71 (1982).

9. A. Smith, P. Guenther, R. Larson, C. Nelson, P. Walker, and J. Whalen, Nucl. Instr. and Methods 50 277 (1967).

10. C. Budtz–Jorgensen, P. Guenther, A. Smith, J. Whalen, W. McMurray, M. Renan, and I. Van Heerden, Z. Phys. 319 47 (1984).

11. P. Guenther, A. Smith, and J. Whalen, Phys. Rev. C12 1797 (1976).

12. Nuclear Standards File IAEA Tech. Report 227, H. Conde, A. Smith and A. Lorenz, Eds., IAEA Press, Vienna (1983).

13. A. Smith, P. Guenther, and R. Sjoblum, Nucl. Instr. and Methods, 140 397 (1977).

14. A. B. Smith, MONTE–SPHERE and MONTE–POLY, Monte–Carlo correction codes, unpublished memoranda (1988), available from the author.

15. W. Poenitz and J. Whalen, Argonne National Laboratory Report, ANL/NDM–80 (1983).

16. A. Smith, P. Lambropoulas, P. Guenther, and J. Whalen, Nucl. Sci. and Eng. 49 389 (1972).

17. See for example: P. E. Hodgson, Nuclear Reactions and Nuclear Structure Clarendon Press, Oxford (1971).

18. D. De Frenne, E. Jacobs, M. Verboven, and G. De Smet, Nuclear Data Sheets 53 73 (1988). See also Table of Isotopes, 7th Edition, C. M. Lederer and V. S. Shirley, Eds., John Wiley and Sons, Inc., New York (1978).

19. A. Gilbert and A. Cameron, Can. J. Phys. 43 1446 (1965).

20. P. A. Moldauer, ANLECIS, private communication (1982).

21. R. L. Walter and P. P. Guss, Proc. Conf. on Nucl. Data for Basic and Applied Science, P. Young, R. Brown, G. Auchampaugh, P. Lisowski, and L. Stewart, Eds., Gordon and Breach, New York, Vol. 2, p. 1079 (1986).

22. S. F. Mughabghab, M. Divadeenam and N. E. Holden, Neutron Cross Sections, Vol. 1, Part A, Academic Press, New York (1980).

23. D. De Frenne, E. Jacobs, M. Verboven, and P. De Gelder, Nuclear Data Sheets 47 261 (1986).

24. Evaluated Nuclear Data File–B, Version V (ENDF/B–V), National Nuclear Data Center, Brookhaven National Laboratory.